

This is a repository copy of *New formation and fate of Isoprene SOA markers revealed by field data-constrained modeling*.

White Rose Research Online URL for this paper:

<https://eprints.whiterose.ac.uk/id/eprint/202042/>

Version: Published Version

---

**Article:**

Zhang, Jie, Liu, Junyi, Ding, Xiang et al. (17 more authors) (2023) New formation and fate of Isoprene SOA markers revealed by field data-constrained modeling. *npj Climate and Atmospheric Science*. 69. ISSN: 2397-3722

<https://doi.org/10.1038/s41612-023-00394-3>

---

**Reuse**

This article is distributed under the terms of the Creative Commons Attribution (CC BY) licence. This licence allows you to distribute, remix, tweak, and build upon the work, even commercially, as long as you credit the authors for the original work. More information and the full terms of the licence here:

<https://creativecommons.org/licenses/>

**Takedown**

If you consider content in White Rose Research Online to be in breach of UK law, please notify us by emailing [eprints@whiterose.ac.uk](mailto:eprints@whiterose.ac.uk) including the URL of the record and the reason for the withdrawal request.

## ARTICLE OPEN



# New formation and fate of Isoprene SOA markers revealed by field data-constrained modeling

Jie Zhang<sup>1,17</sup>, Junyi Liu<sup>2</sup>, Xiang Ding<sup>3,4</sup>, Xiao He<sup>5</sup>, Tianle Zhang<sup>6</sup>, Mei Zheng<sup>2</sup>, Minsu Choi<sup>1</sup>, Gabriel Isaacman-VanWertz<sup>6</sup>, Lindsay Yee<sup>7</sup>, Haofei Zhang<sup>8</sup>, Pawel Misztal<sup>9</sup>, Allen H. Goldstein<sup>10</sup>, Alex B. Guenther<sup>10</sup>, Sri Hapsari Budisulistiorini<sup>11</sup>, Jason D. Surratt<sup>11</sup>, Elizabeth A. Stone<sup>12</sup>, Manish Shrivastava<sup>13</sup>, Dui Wu<sup>14,15</sup>, Jian Zhen Yu<sup>5,16</sup>✉ and Qi Ying<sup>1</sup>✉

Particulate 2-methyltetrols (2-MT) and 2-methylglyceric acid (2-MG) are typically used to indicate the abundance of isoprene-derived secondary organic aerosols (SOA). However, their formation and fate are not fully understood. In this study, we showed that particulate 2-MT and 2-MG collected at multiple monitoring sites under a wide range of atmospheric and emission conditions, with concentrations spanning six orders of magnitudes, are well reproduced with an expanded isoprene-SOA scheme implemented into the Community Multiscale Air Quality (CMAQ) model. The scheme considers their three-phase (gas-aqueous-organic phase) partitioning, formation from acid-driven multiphase reactions, and degradation by OH radicals in the gas and aqueous phases. The model results reveal that a non-aqueous formation pathway or direct biogenic emission is needed to supplement the commonly assumed acid-driven multiphase reaction process to explain the observed 2-MT concentrations. This missing pathway contributes to 20–40% of 2-MT in areas with aerosol pH < 2 and more than 70% under less acidic conditions (pH ~ 2–5), such as those encountered in the western US and China. The typical summertime gas-phase photochemical lifetimes of 2-MT and 2-MG are estimated to be 4–6 and 20–30 h, respectively, and their aqueous lifetimes are approximately 20–40 h. Our simulations show that predicted 2-MT is mainly influenced by its aqueous phase loss to OH, but 2-MG is more sensitive to gas phase OH loss due to the preferential partitioning of the two tracers in the aqueous and gas phases, respectively.

*npj Climate and Atmospheric Science* (2023)6:69; <https://doi.org/10.1038/s41612-023-00394-3>

## INTRODUCTION

Isoprene is the most abundant nonmethane biogenic volatile organic compound (VOC) emitted into the atmosphere, with estimated annual global emissions of 500–750 Tg<sup>1</sup>. It is highly reactive and can be oxidized by hydroxyl radical (OH)<sup>2,3</sup>, ozone (O<sub>3</sub>)<sup>4</sup>, and nitrate radical (NO<sub>3</sub>)<sup>5</sup> to generate semivolatile and low-volatile organic aerosol products<sup>6–10</sup>. In areas with larger isoprene emissions, such as the Eastern United States (US), isoprene contributes to more than 45% of the summertime secondary organic aerosol (SOA)<sup>11</sup>.

The chemical composition of isoprene SOA has been extensively investigated in chamber experiments and modeling studies<sup>9,10,12,13</sup>. Among the identified isoprene SOA species, 2-methyltetrols (2-MT, including 2-methylthreitol and 2-methylerythritol)<sup>14</sup> and 2-methylglyceric acid (2-MG) are considered unique tracer compounds<sup>15,16</sup>, and have been widely used to estimate the overall isoprene-derived SOA in field studies<sup>17,18</sup>. Immediate precursors of 2-MT and 2-MG were found to be water-soluble products, i.e., isoprene epoxydiols (IEPOX) from isoprene OH

oxidation under low-NO<sub>x</sub> conditions<sup>9,19</sup>, and methacrylic acid epoxide (MAE) and hydroxymethyl-methyl- $\alpha$ -lactone (HMML) formed under high-NO<sub>x</sub> conditions<sup>10,20</sup>, respectively. Formation of 2-MT and 2-MG is thought to occur mainly in the highly acidic aerosol water through irreversible surface uptake of IEPOX and MAE/HMML, respectively<sup>9,10,21,22</sup>. Based on these studies, Pye et al.<sup>23</sup> and Budisulistiorini et al.<sup>24</sup> implemented a multiphase reaction scheme in a regional chemical transport model to explicitly predict the generation of 2-MT and 2-MG in aerosol water.

However, 2-MT and 2-MG have also been detected in the aerosol phase under dry conditions and in laboratory-generated non-acidic seed aerosols<sup>15,16,25–27</sup>. 2-MT has been proposed to be primarily emitted in the gas phase due to biological processes and environmental stressors<sup>28</sup>, and its convective updraft and gas-particle partitioning were shown to explain upper tropospheric aircraft measurements of IEPOX-SOA over the Amazon rainforest<sup>29</sup>. These studies suggest the potential existence of non-aqueous pathways for 2-MT from isoprene. Although

<sup>1</sup>Zachary Department of Civil and Environmental Engineering, Texas A&M University, College Station, TX 77845, USA. <sup>2</sup>State Key Joint Laboratory of Environmental Simulation and Pollution Control, College of Environmental Sciences and Engineering, Peking University, Beijing 100871, China. <sup>3</sup>State Key Laboratory of Organic Geochemistry and Guangdong Provincial Key Laboratory of Environmental Protection and Resources Utilization, Guangzhou Institute of Geochemistry Chinese Academy of Sciences, Guangzhou 510640, China. <sup>4</sup>Guangdong-Hong Kong-Macao Joint Laboratory for Environmental Pollution and Control, Guangzhou Institute of Geochemistry, Chinese Academy of Science, Guangzhou 510640, China. <sup>5</sup>Division of Environment & Sustainability, Hong Kong University of Science & Technology, Clear Water Bay, Kowloon, Hong Kong 999077, China. <sup>6</sup>Department of Civil and Environmental Engineering, Virginia Polytechnic Institute and State University, Blacksburg, VA 24061, USA. <sup>7</sup>Department of Environmental Science, Policy and Management, University of California, Berkeley, CA 94720, USA. <sup>8</sup>Department of Chemistry, University of California, Riverside, CA 92521, USA. <sup>9</sup>Department of Civil, Architectural and Environmental Engineering, University of Texas at Austin, Austin, TX 78712, USA. <sup>10</sup>Department of Earth System Science, University of California, Irvine, CA 92697, USA. <sup>11</sup>Department of Environmental Sciences and Engineering, University of North Carolina at Chapel Hill, Chapel Hill, NC 27599, USA. <sup>12</sup>Department of Chemistry, University of Iowa, Iowa City, IA 52242-1294, USA. <sup>13</sup>Pacific Northwest National Laboratory, Richland, WA 99352, USA. <sup>14</sup>Institute of Mass Spectrometry and Atmospheric Environment, Guangdong Provincial Engineering Research Center for On-line Source Apportionment System of Air Pollution, Jinan University, Guangzhou 510632, China. <sup>15</sup>Guangdong-Hongkong-Macau Joint Laboratory of Collaborative Innovation for Environmental Quality, Guangzhou 510632, China. <sup>16</sup>Department of Chemistry, Hong Kong University of Science & Technology, Clear Water Bay, Kowloon, Hong Kong 999077, China. <sup>17</sup>Present address: Pacific Northwest National Laboratory, Richland, USA. ✉email: [jian.yu@ust.hk](mailto:jian.yu@ust.hk); [qying@civil.tamu.edu](mailto:qying@civil.tamu.edu)

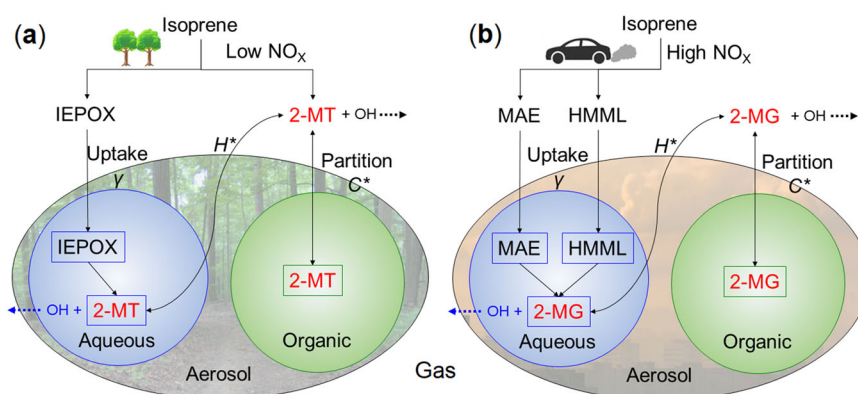


**Fig. 1 Schematic of the formation, partitioning, and photochemical decay of isoprene SOA tracers. a** 2-methyltetrols (2-MT). **b** 2-methylglyceric acid (2-MG).

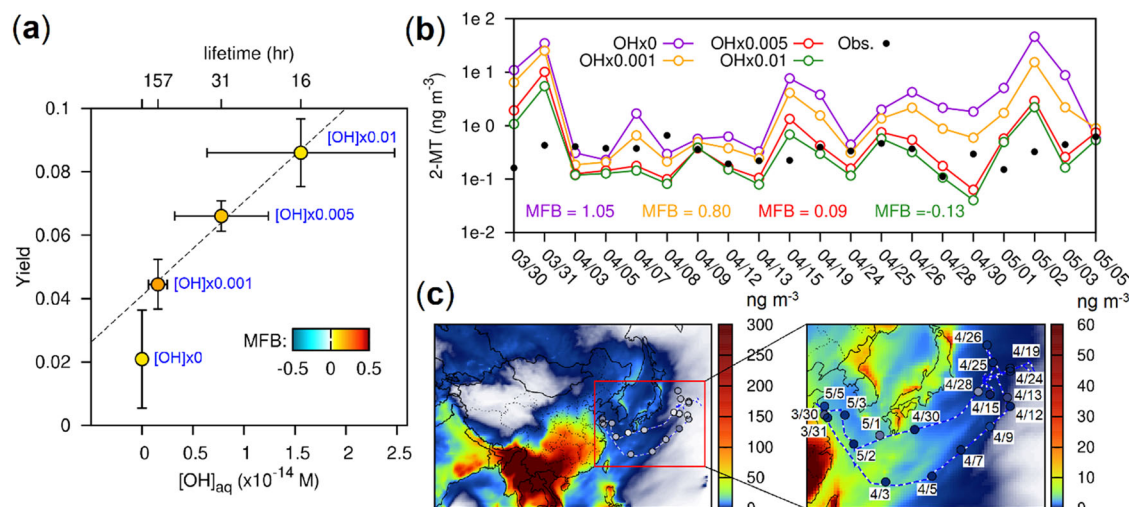


**Fig. 2 Mass yield and predicted 2-MT for four different  $[OH]_{aq}$  scaling factors. a** Estimated 2-MT mass yield from the additional non-aqueous pathway for four different  $[OH]_{aq}$  scaling factors. The x-axis is the modeled average daily  $[OH]_{aq}$  concentrations at the SOAS and PRD monitoring sites. The data points are colored by the mean fraction bias (MFB) of the predicted daily 2-MT at those monitoring sites. Uncertainties for the OH radical concentrations are one standard deviation of the daily concentrations. Uncertainties of the mass yield are based on the Monte Carlo analysis assuming that the measured and predicted 2-MT from the multiphase phase formation pathway has a 20% relative uncertainty. **b** Predicted and observed daily average 2-MT concentrations along the cruise tracks **(c)**.

Budisluistorini et al. showed that the two tracers could be reasonably estimated solely from the acid-driven multiphase reactions, their treatment of the two tracers as non-volatile and non-reactive species might compensate for the potentially missing non-aqueous pathways<sup>23,30</sup>. In reality, the tracers have been detected in significant amounts in gas and particle phases in field experiments, suggesting both species are likely semivolatile<sup>31–33</sup>. Additionally, the 2-MT and 2-MG oxidation reactions with OH radicals in the gas and aqueous phase could be effective removal pathways, which have not been considered in modeling studies<sup>28,34–36</sup>.

In this study, we expand the regional isoprene SOA scheme of Pye et al.<sup>23</sup> implemented in the Community Multiscale Air Quality (CMAQ) model to simulate the formation of 2-MT and 2-MG by treating these two species as semivolatile with gas-aqueous-organic three-phase partitioning. Photochemical losses of the two species in gas and aerosol phases by OH radicals are fully considered for the first time. We also consider the non-aqueous formation of 2-MT from isoprene, as described in Fig. 1. Modeled 2-MT and 2-MG concentrations in the US and China compared well with measurements from the Southern Oxidant and Aerosol Study (SOAS), the field campaign in the Pearl River Delta (PRD) region in summer, and the West Pacific Ocean on a cruise ship

(R/V Dongfanghong II) in spring, ranging six orders of magnitudes. Observed gas-particle partitioning of the two species in SOAS was also well reproduced. Our model results, constrained by the observation data, provide solid evidence for the existence of non-aqueous 2-MT formation pathways, in addition to the widely used acid-driven multiphase reaction process. In addition, our results showed that gas-particle partitioning and photochemical removal are important processes that affect the particulate concentrations of the two tracers. To the best of our knowledge, this is the first regional modeling study to estimate the photochemical lifetime of 2-MT and 2-MG in gas and aerosol aqueous phases.

## RESULTS

### 2-MT non-aqueous pathway mass yield and its photochemical lifetime

The photochemical lifetime of 2-MT and 2-MG in the aqueous phase is determined by the 2<sup>nd</sup> order reaction rate coefficients ( $k_{aq,2-MT} = 1.14 \times 10^9 \text{ M}^{-1} \text{ s}^{-1}$  and  $k_{aq,2-MG} = 0.97\text{--}1.41 \times 10^9 \text{ M}^{-1} \text{ s}^{-1}$ )<sup>35,36</sup> and the modeled OH radical concentrations in the aerosol water ( $[OH]_{aq}$ ). As discussed in Supplementary Note 2: *The formation, gas-particle partitioning, and removal of 2-MT and 2-MG*,  $[OH]_{aq}$  is estimated from

**Table 1.** Important parameters for simulating 2-MT and 2-MG in the model and estimated lifetime of 2-MT and 2-MG in the gas and the aerosol aqueous phase.

Parameters for simulating 2-MT and 2-MG						
		2-MT		2-MG		
$C^*$ at 298 K ( $\mu\text{g m}^{-3}$ )		14.6		30.3		
$\Delta H_{\text{vap}}$ (kJ mol $^{-1}$ )		117.7		130.0		
$H^*$ at 298 K (M atm $^{-1}$ )		$3.38 \times 10^{10}$		$5.25 \times 10^8$		
$k_{\text{OH,gas}}$ (cm $^3$ molecule $^{-1}$ s $^{-1}$ )		$3.66 \times 10^{-11}$		$6.87 \times 10^{-12}$		
$k_{\text{OH,aq}}$ (M $^{-1}$ s $^{-1}$ )		$1.14 \times 10^9$		$0.97\text{--}1.41 \times 10^9$ <sup>a</sup>		
Average conc.		2-MT		2-MG		
		lifetime (h)		lifetime (h)		
	OH gas (10 $^6$ molec. cm $^{-3}$ )	OH aqueous (10 $^{-14}$ M)	Gas	Aq.	Gas	Aq.
Typical	1.00	1.00	7.6	24.4	13.5 <sup>b</sup> (40.4) <sup>c</sup>	27.8
SOAS	1.23	0.71	6.2	34.1	11.0 (32.9)	38.9
PRD	1.75	0.78	4.3	31.4	7.7 (23.1)	35.8
West Pacific	1.19	1.11	6.4	22.0	11.3 (34.0)	25.0
China <sup>d</sup>	1.87	1.16	4.1	21.0	7.2 (21.6)	23.9

<sup>a</sup>The  $k_{\text{OH,aq}}$  for 2-MG is pH dependent,  $k_{\text{OH,aq}} = 9.7 \times 10^8 \text{ M}^{-1} \text{ s}^{-1}$  at pH = 2;  $k_{\text{OH,aq}} = 1.41 \times 10^9 \text{ M}^{-1} \text{ s}^{-1}$  at pH = 5.

<sup>b</sup>based on higher reaction rate  $k_{\text{g,2-MG}} = 2.06 \times 10^{-11} \text{ cm}^3 \text{ molecule}^{-1} \text{ s}^{-1}$  in the sensitive study.

<sup>c</sup>based on  $k_{\text{g,2-MG}} = 6.87 \times 10^{-12} \text{ cm}^3 \text{ molecule}^{-1} \text{ s}^{-1}$  in the base case simulation.

<sup>d</sup>Average OH radical concentrations at 14 sites.

the equilibrium partitioning of modeled gas-phase OH radicals and adjusted by a scaling factor to account for the net effect of OH formation and loss in the aqueous phase<sup>37</sup>. A scaling factor of zero indicates that no aqueous source/sink of OH is needed. The three non-zero scaling factors (0.001, 0.005, and 0.01) are selected to cover the possible range of reported  $[\text{OH}]_{\text{aq}}$  from previous studies (see Supplementary Note 2)<sup>35,36,38,39</sup>. The 2-MT from the non-aqueous formation pathway (Fig. 1a) is assumed to form predominantly from isoprene oxidation under low-NO<sub>x</sub> condition (i.e., from  $\text{ISOPO}_2 + \text{HO}_2$ ) using a mass-yield approach. The mass yield of 2-MT (i.e., gram of 2-MT formed per mole of  $\text{ISOPO}_2$  reacted with  $\text{HO}_2$ ) is determined by fitting the modeling results with daily field measurements in the SOAS and PRD regions. Figure 2a shows that four scaling factors investigated in this study lead to positive mass yields (a) of 2-MT from the additional non-aqueous pathway, ranging from  $0.021 \pm 0.02$  ( $[\text{OH}]_{\text{aq}} = 0$ ) to  $0.086 \pm 0.01$  for  $[\text{OH}]_{\text{aq}} < 0.01$ , which corresponds to an average predicted daily  $[\text{OH}]_{\text{aq}}$  of  $\sim 1.5 \times 10^{-14} \text{ M}$  at the SOAS and PRD monitor sites.

The mass yields and the average photochemical lifetime of aqueous-phase 2-MT (16–157 h,  $k_{\text{aq,2-MT}} = 1.14 \times 10^9 \text{ M}^{-1} \text{ s}^{-1}$ )<sup>36</sup> are further constrained using the 2-MT observations along the cruise track in the Asian continental outflow impacted regions over the Western Pacific. The predicted 2-MT in this region is affected by the long-range transport from high isoprene emission areas in East and Southeast Asia and direct ocean emissions of isoprene, as shown in Fig. 2c. The 2-MT predictions in the outflow region are highly sensitive to  $[\text{OH}]_{\text{aq}}$ . Figure 2b shows that the predictions with  $[\text{OH}]_{\text{aq}}$  adjusted by a scaling factor of 0.005 (hereafter OH $\times 0.005$ ) with a corresponding non-aqueous pathway mass yield of  $0.066 \pm 0.005$  have the best agreement with the observations with a mean fractional bias (MFB, Supplementary Equation 18) of 0.09. The sensitivity tests with different OH concentrations for the aqueous loss process greatly affect

predicted 2-MT from April 15<sup>th</sup> to May 5<sup>th</sup>. During this period, the cruise encountered outflow from the land, which experienced several days of gas and aqueous phase aging with OH radicals. In contrast, from April 3<sup>rd</sup>–13<sup>th</sup>, the cruise traveled over the southern part that only experienced local clean marine emissions and was less affected by continental outflow. During this time, aqueous photochemical decay did not affect 2-MT concentrations much since 2-MT was mostly locally formed from the marine isoprene emissions. Inclusion of this additional non-aqueous pathway within the model was also found to greatly reduce the model-measurement gaps in 2-MT concentrations at the SOAS sites in the US and the PRD sites in southern China. In addition, the independent measurements from Western Pacific were used to evaluate the necessity of the non-aqueous formation pathway. The MFB = 0.14 and R = 0.40 with the inclusion of this additional pathway are much improved compared to the default MFB = −0.33 and R = 0.33 without the additional non-aqueous pathway using this mass yield and  $[\text{OH}]_{\text{aq}}$  scaling factor.

Corresponding to the predicted  $[\text{OH}]_{\text{aq}}$  in OH $\times 0.005$ , the 2-MT lifetime in the aerosol aqueous phase is  $\sim 20$  h over the Western Pacific Ocean in spring and  $\sim 30$ –35 h at the SOAS and PRD sites in summer, as summarized in Table 1. The 2<sup>nd</sup>-order rate coefficients for 2-MT with OH in the gas phase ( $k_{\text{g,2-MT}}$ ) estimated from the three methods are consistent with each other ( $2.5 \sim 4.9 \times 10^{-11} \text{ cm}^3 \text{ molecule}^{-1} \text{ s}^{-1}$ , see Supplementary Table 3). In the above simulations, an average value of  $3.66 \times 10^{-11} \text{ cm}^3 \text{ molecule}^{-1} \text{ s}^{-1}$  is used, which leads to lifetimes of  $\sim 4.3$ – $6.4$  h in the gas phase (Table 1). Although the lifetime of 2-MT in the gas phase is shorter than its lifetime in the aqueous phase, sensitivity simulations show that the predicted concentrations are not sensitive to the gas phase decay because most of the 2-MT is in the particle phase, as discussed in 2-MT and 2-MG phase distribution and formation pathways.

### The photochemical lifetime of 2-MG

The aqueous photochemical lifetime of 2-MG is close to that of 2-MT, approximately 25–40 h based on OH $\times 0.005$ . The 2-MG predictions along the cruise track show little variation due to different aqueous OH concentrations, as shown in Supplementary Fig. 13 because only a small fraction of 2-MG exists in the aqueous phase (less than 10%, as shown in Supplementary Fig. 15). However, the 2-MG gas-phase reaction rate coefficient ( $k_{\text{g,2-MG}}$ ) estimations have a wide range of  $2.36 \sim 13.7 \times 10^{-12} \text{ cm}^3 \text{ molecule}^{-1} \text{ s}^{-1}$ . In this work, we applied the average value ( $k_{\text{g,2-MG}} = 6.87 \times 10^{-12} \text{ cm}^3 \text{ molecule}^{-1} \text{ s}^{-1}$ ) of the three estimations in Table 1 for the base case simulation (a list of cases simulated is shown in Supplementary Table 4) and assessed the uncertainty of  $k_{\text{g,2-MG}}$  in 2-MG predictions by scaling up or down its value by a factor of 3 to cover the entire range of the estimated rate coefficients.

The predicted particle-phase 2-MG concentrations along the cruise track are approximately a factor of 2 higher than the observations (MFB = 0.67) in the base case. The simulation with the upper limit of reaction rate coefficient ( $k_{\text{g,2-MG}} = 2.06 \times 10^{-11} \text{ cm}^3 \text{ molecule}^{-1} \text{ s}^{-1}$ ) shows better overall agreement with the observations (MFB = 0.13) (see Supplementary Fig. 14a). Despite the obvious large impact on 2-MG concentrations in the outflow region, Supplementary Fig. 14c shows that the uncertainties in the estimated  $k_{\text{g,2-MG}}$  on the predicted 2-MG concentrations are small (within  $\pm 25\%$ ) at the isoprene emission impacted SOAS and PRD sites. The base case predictions show the best agreement with observations at Centreville (CTR) and PRD sites, but it is over-predicted at the Look Rock (LRK) site. Based on these results,  $k_{\text{g,2-MG}}$  is likely within  $6.87 \times 10^{-12}$  and  $2.06 \times 10^{-11} \text{ cm}^3 \text{ molecule}^{-1} \text{ s}^{-1}$ , but additional laboratory studies are needed to reduce the uncertainty in this important parameter. The summertime lifetimes of 2-MG in the gas phase at the SOAS and PRD sites are 11–33 and 8–23 h, respectively. The lifetime of 2-MG along the cruise track in



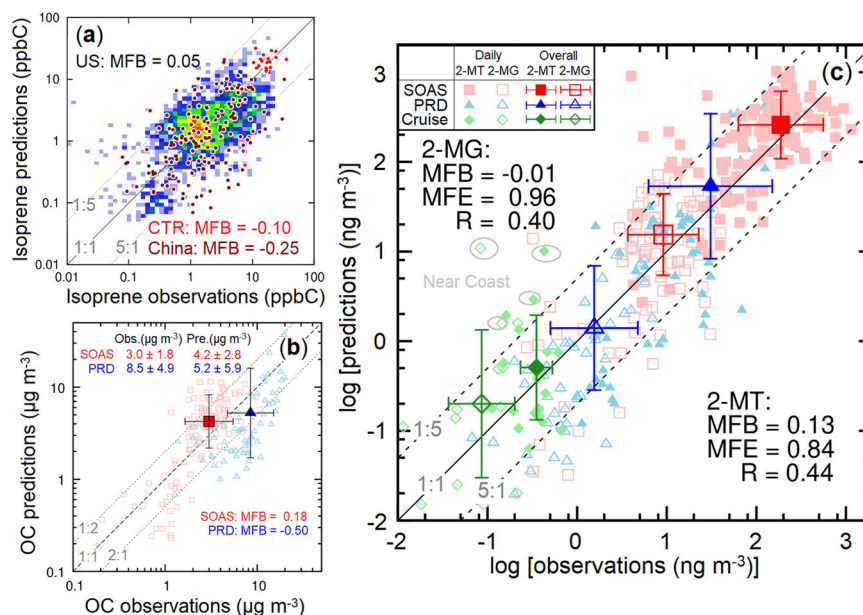


**Fig. 3 Model evaluation of isoprene, organic carbon (OC), 2-MT, and 2-MG.** **a** Daily isoprene concentrations at the monitoring sites in the US (background density scatter plot – PAMS data; red dots – CTR SOAS site data) and China (brown dots). **b** Daily organic carbon (OC) at the CTR site and the PRD sites (Supplementary Fig. 1) sites. **c** 2-MT and 2-MG daily (light color dots) and campaign average concentrations (points with error bars) at multiple SOAS (CTR, LRK, and RTP) and PRD sites, and along the cruise tracks (Cruise, Fig. 1c). The predictions are based on the OH $\times$ 0.005 case (Base Case in Supplementary Table 4). The locations of the PAMS stations and the CTR site are shown in Supplementary Fig. 6a and Supplementary Fig. 1, respectively. The locations of the isoprene monitoring sites in China are shown in Supplementary Fig. 6b. Error bars represent one standard deviation of the daily concentrations.

the West Pacific in spring is  $\sim 11\text{--}34$  h, as summarized in Table 1. We find no clear indication of missing sources of 2-MG under ambient conditions investigated in this study (overall MFB =  $-0.01$  and  $R = 0.40$ , as shown in Fig. 3c).

### 2-MT and 2-MG phase distribution and formation pathways

The predictions in the base case (OH $\times$ 0.005,  $\alpha = 0.066$ ,  $k_{g,2\text{-MG}} = 6.87 \times 10^{-12} \text{ cm}^3 \text{ molecule}^{-1} \text{ s}^{-1}$ ) are more thoroughly evaluated. The evaluation of isoprene mixing ratio and organic carbon (OC) is discussed in Supplementary Note 4, and shown in Fig. 3a, b. The model predicted aerosol pH agrees well with that derived from ISORROPIA based on measured aerosol composition in SOAS and West Pacific Ocean. The daily 2-MT and 2-MG predictions at the SOAS and PRD sites and over the open ocean are mostly within a factor of 5 of the observations in a wide concentration range across six orders of magnitudes ( $10^{-2}$  to  $10^3 \text{ ng m}^{-3}$ , see Fig. 3c). There is no significant bias for daily 2-MT and 2-MG predictions (MFB = 0.13 and  $-0.01$ , respectively) with a moderate Pearson correlation ( $R = 0.44$  and  $0.40$ , respectively). 2-MT is slightly overpredicted at the SOAS sites (MFB = 0.32) but underpredicted at the PRD sites (MFB =  $-0.23$ ). The 2-MG at the SOAS sites is well captured (MFB = 0.14). Although 2-MG is slightly underpredicted in the PRD region (MFB =  $-0.51$ ), the correlation between daily observations and predictions is strong ( $R = 0.71$ ). Systematic differences in the observed concentrations could partially contribute to the variation in model performance statistics among different data sets because data collection and measurements were performed using different methods<sup>40–42</sup>.

The average isoprene tracer concentrations at SOAS sites are significantly higher than those from the PRD sites, but the phase distributions are similar, as shown in Supplementary Fig. 15a. 2-MT is mainly partitioned into the particle phase (daily average 74–78%), and approximately 70% of the total 2-MT is in the aqueous phase at both SOAS and PRD sites. In contrast, 2-MG is mostly in the gas phase (only 18–25% in the particle phase) due to the lower Henry's law constant, higher saturation mass

concentration (Table 1), and low aerosol pH. Moreover, the fraction of 2-MG in the aqueous phase is lower than that in the organic phase. The similar phase distribution is related to the environmental conditions between the southeast US and the PRD region in China (see Supplementary Fig. 16). The estimated Henry's Law constants ( $H^*$ ) vary over several orders of magnitude for both species. Uncertainties in the predicted 2-MT and 2-MG are investigated in Supplementary Discussion: *Uncertainty in tracer predictions due to gas-aqueous partitioning*. In summary, particle phase and total concentrations of 2-MG are not very sensitive to  $H^*$ , but 2-MT predictions show higher sensitivity to the  $H^*$  value.

In this work, 2-MT is formed from the IEPOX multiphase chemical pathway and the additional non-aqueous pathway, and contributions from each pathway are tracked separately. As shown in Supplementary Fig. 12b, the non-aqueous pathway contributes up to 15–40% to the 2-MT predictions at SOAS and PRD sites. The higher contributions correspond to higher estimated  $[\text{OH}]_{\text{aq}}$  as more non-aqueous formation is required to compensate for the higher aqueous-phase removal of 2-MT by OH radicals. The 2-MG is formed from the multiphase oxidation pathway of HMML and MAE in the model. The HMML pathway is the major contributor based on the updated gas chemistry mechanism, accounting for 70–80% of the total 2-MG. This agrees with the recent observation analysis<sup>41,43</sup>. The regional distributions of 2-MG formed from HMML and MAE pathways are similar, as shown in Supplementary Fig. 17.

Figure 4 shows the relative contribution from the non-aqueous pathway to the predicted 2-MT in the US and China. In the high concentration areas (i.e., Southeast US and Southern China), 2-MT is mainly formed by the multiphase chemical reactions of IEPOX (also see Supplementary Fig. 18). Approximately 10–30% is generated from the non-aqueous pathway, caused by the low aerosol pH ( $\text{pH} = 1\text{--}2$  in the southeast US and  $\text{pH} = 2\text{--}3$  in southern China). The contribution from the non-aqueous pathway becomes more than 70% in the less-acidic regions in the western US and China, where  $\text{pH} = 4\text{--}6$  due to alkaline elements from windblown dust<sup>44–46</sup>.

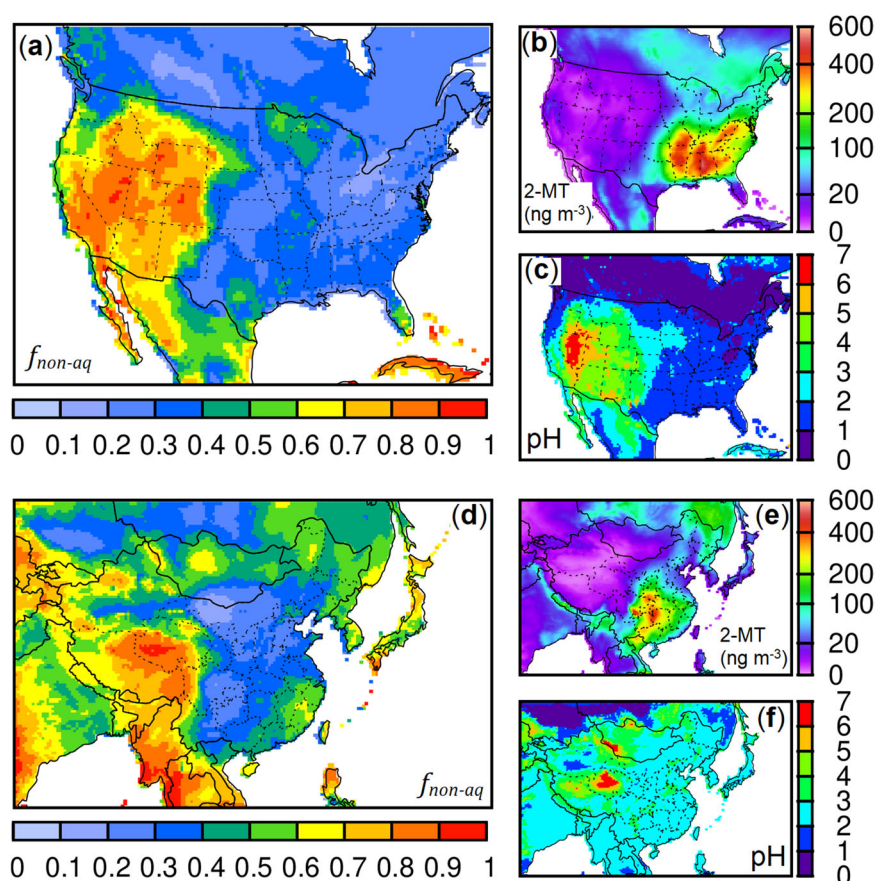


**Fig. 4** Relative contributions of non-aqueous pathway to 2-MT. **a, d** Fraction of predicted 2-MT from the non-aqueous pathway ( $f_{\text{non-aq}}$ ). **b, e** Total concentrations of 2-MT ( $\text{ng m}^{-3}$ ). **c, f** Aerosol pH in the US and in China for the  $\text{OH} \times 0.005$  case (Base Case in Supplementary Table 4).

It should be noted that 2-MT formation in the gas phase reactions is one possible way to explain the underestimation of 2-MT from the multiphase chemical pathway alone. Direct emissions of 2-MT might also explain the missing 2-MT<sup>29</sup>. As shown in Supplementary Fig. 19, using a molar emission ratio of 2-MT to isoprene of 0.54%, the direct emissions of 2-MT lead to similar 2-MT concentrations as the assumed formation from the gas phase oxidation with  $\alpha = 0.066$ . It is also possible that the additional 2-MT is not directly emitted but due to reactions of low volatility oxidation products from isoprene (e.g., multifunctional peroxides) within the canopy. Additional evidence from both the field study (e.g., spatial distributions of 2-MT, as in Ye et al.<sup>28</sup>) and the chemical mechanism sides is needed to further clarify this. The potential uncertainties on IEPOX uptake coefficient due to particle phase separation is analyzed in Supplementary Discussion: *Uncertainty on IEPOX uptake coefficient due to the particle phase separation*. In addition, some recent studies suggested that GC/MS-based measurements might potentially lead to biased high 2-MT due to reactions that form 2-MT during the analyses<sup>47–49</sup>. The impacts of this analytical uncertainty on  $\alpha$  are discussed in Supplementary Discussion: *Uncertainty in the analytical artifacts of 2-MT measurements*.

Isoprene-SOA tracers (i.e., 2-MT and 2-MG) and other formed SOA compounds are more significant during the summertime when isoprene emitted from biogenic sources is at its highest<sup>18</sup>. Based on previous study in the southeast US, the aerosol water is relatively lower in winter, and the aerosol pH is higher by  $\sim 1$  unit than that in summer<sup>50</sup>. These will reduce the 2-MT and 2-MG formed through multiphase acid-driven reactions. Therefore, the 2-MT formation from the additional non-aqueous phase pathway suggested in this study could become more important during the

wintertime. However, further observations of the isoprene SOA tracers, especially in winter/spring seasons are needed to support modeling studies of the seasonal variability of the 2-MT formation pathways.

#### 2-MT model predictions from the additional and multiphase pathways in China

The SOAS and PRD field campaigns are at locations with high isoprene emissions and acidic aerosols, so the relative contributions from the multiphase chemical pathway of IEPOX to 2-MT are high. To further evaluate the capability of our model in broad areas with a wide range of atmospheric and emission conditions, we simulated 2-MT at 14 sites across China from June to August 2012 and compared our predictions with particle-phase 2-MT measurements reported by Ding et al.<sup>42</sup> (Supplementary Fig. 20). Predicted 2-day average 2-MT concentrations are approximately a factor of 2 lower than observations ( $\text{MFB} = -0.85 \sim -0.60$ ), but they show a very strong correlation ( $R > 0.7$ ). The larger under-predictions at the Nam Co and Dunhuang sites are at least partially related to the under-estimations of isoprene emissions from local sources at the two sites<sup>51,52</sup>. As shown in Supplementary Fig. 20a, the fractional contribution of the additional non-aqueous pathway at monitoring sites in Eastern China is generally lower than 50%. However, the non-aqueous formation becomes a dominant pathway for the sites in Western China, i.e., Xishuangbanna, Linzhi, and Sanya, where the estimated aerosol pH is higher than that at other sites. The strong correlation between observations and predictions shows that our model with the additional 2-MT formation from the non-aqueous pathway can predict 2-MT under a wider range of aerosol acidity conditions.

### Optimizing the gas-particle partitioning of 2-MG

The predicted particle fraction ( $F_{pt}$ ) of 2-MT and its diurnal variations (0.6–0.85) during SOAS at the CTR site agree well with observed gas-particle partitioning (see Supplementary Fig. 21b) using the thermal desorption aerosol gas chromatography (SV-TAG)<sup>32</sup>. For 2-MG, predicted  $F_{pt}$  values (0.1–0.4) are consistently lower than observed values at all hours (0.4–0.6), with larger discrepancies occurring during the day. The predicted total and particle-phase 2-MG concentrations are higher than the observations, although they agree well with the filter-based measurements.

Since a large fraction of 2-MG is in the gas phase, and the particle phase concentrations are low, filter-based measurements may be subject to biases from sampling (e.g., adsorption of gas-phase 2-MG on filters) and analysis (e.g., formation from other species during thermal desorption). In comparison, the SV-TAG measured particle-phase concentrations, sampled with a carbon denuder placed upstream and for a much shorter duration<sup>32</sup>, are expected to be more accurate than the filter-based measurements. Through trial and error, we determined a set of adjustments that led to better agreements in the total concentrations (Supplementary Fig. 21c, 21d) and the gas-particle partitioning (Supplementary Fig. 21a). In addition, the predicted average particle-phase 2-MG at the LRK site also agrees better with the filter-based observation (Supplementary Fig. 21e). Details of the changes in the related parameters are shown in Table 1. Since most of the data used in this study are filter-based and more careful comparisons are needed between the filter-based and SV-TAG data, we refrain from adopting these adjustments in the base case model result. Additional evaluation of the model predictions against more SV-TAG measurements is needed to confirm or refute them in future studies.

### DISCUSSION

Most previous modeling studies of 2-MT and 2-MG formation are limited to the multiphase reactions followed by the irreversible reactive surface uptake of IEPOX and HMML/MAE, respectively, while the volatility, removal processes, and the possibility of other formation pathways are not considered. Under ambient air conditions, the three-phase partitioning scheme distributes a large fraction of 2-MT in the particle phase and 2-MG in the gas phase. The partitioning equilibrium is important due to different photochemical lifetimes estimated based on the reactions with OH radicals in the particle and gas phases. The influence of the removal processes could cause large variations in the predicted concentrations by several orders of magnitude in remote regions.

The photochemical lifetime of 2-MT in the particle phase depends on the OH radical concentrations in the aerosol water. Our modeling investigation suggests that the reasonable aqueous-phase 2-MT lifetime could be ~25 h when  $[OH]_{aq}$  is approximately  $1 \times 10^{-14}$  M. The value of  $k_{g,2-MG} = 6.87 \times 10^{-12}$  cm<sup>3</sup> molecule<sup>-1</sup> s<sup>-1</sup> leads to reasonable agreement between 2-MG predictions and observations under various atmospheric conditions. However, the uncertainty in the rate coefficient needs to be further reduced in future studies.

When the removal processes of 2-MT are included in the model, predicted 2-MT concentrations from the multiphase chemical reactions of IEPOX alone are biased low. The inclusion of an additional non-aqueous formation pathway is found to offset the systematic under-predictions of 2-MT, especially in areas with lower aerosol acidity. In addition, this additional pathway may be able to explain the formation of 2-MT in smog chamber experiments with non-acidic seed particles and under dry conditions, although some of the 2-MT seen in these experiments might be an analytical artifact originated from the reactions of the organic peroxides during the GC/MS analysis<sup>53</sup>. In this study, we

found that the estimated 2-MT primary emission rate based on the modeled non-aqueous 2-MT from gas-phase chemistry was close to the 2-MT primary emission rate proposed in Shrivastava et al.<sup>29</sup> over the Amazon. While further experimental and modeling studies are still needed to elucidate the actual chemical mechanism of this non-aqueous 2-MT formation pathway, it is clear that this additional source is needed to explain observations in a variety of locations. In addition, using unique cruise observations, our study shows that the photochemical loss processes of 2-MT with OH radicals in the aqueous phase are important processes that reduce model-measurements gaps by orders of magnitude corresponding to the continental outflow over oceans.

### METHODS

#### Observation data

The 2-MT and 2-MG observation data includes field measurements from campaigns including the SOAS<sup>54</sup>, the PRD region of China<sup>55</sup>, the 14 inland sites in China<sup>42</sup>, and the West Pacific Ocean. Aerosols were collected on quartz fiber filters at three SOAS monitoring sites (i.e., CTR, LRK, and RTP) from June 1st to July 15th, 2013, and the samples were analyzed using GC/MS<sup>24,56</sup>. In addition to the filter-based measurements, hourly SV-TAG measurements at the CTR site were used to evaluate the modeled gas-particle partitioning of 2-MT and 2-MG. While the SOAS sites are located in the rural area of the southeast US, the 4 monitoring sites in the PRD region of China are located in urban, suburban, and industrial areas. 24 h PM<sub>2.5</sub> samples were collected on quartz filters and analyzed by an Agilent GC-MSD system in summer of 2012<sup>55,57,58</sup>. During the same time, tracer concentrations at other 14 sites across China with large variation of isoprene emissions and atmospheric conditions were measured by the same method, as reported by Ding et al.<sup>42</sup>. The cruise ship (R/V Dongfanghong II) was traveling along the outflow impacted region in the West Pacific Ocean and collected PM<sub>2.5</sub> filter samples during the spring of 2015. The preprocessing and analytical methods are found in Zhang et al.<sup>40</sup> and Ding et al.<sup>18</sup>.

The site locations, detailed descriptions, and quantification methods can be found in the Supplementary Note 1: *Field measurement data of 2-MT and 2-MG*.

#### Model development and application

The 2-MT and 2-MG schemes developed in this study include gas-particle partitioning, gas and multiphase formation, and photochemical decay processes. Their equilibrium partitioning between the gas, aqueous and organic phases follows a similar three-phase partitioning approach described by Griffin et al.<sup>59</sup>. The gas-organic phase partitioning equilibrium is described by the absorptive gas-organic matter (OM) partitioning coefficient<sup>60</sup>, and the gas-aqueous phase partitioning equilibrium is described by Henry's Law.

The multiphase chemical formation of 2-MT and 2-MG in the aerosol water<sup>23</sup> and an additional non-aqueous formation pathway of 2-MT in the gas phase from isoprene low-NO<sub>x</sub> oxidation using a mass-yield approach are implemented in the model<sup>28</sup>, as shown in Fig. 1. The optimal mass yield of 2-MT from this non-aqueous pathway is determined by a modified multilinear regression approach using an objective function with log-normal error suggested by Liao et al.<sup>61</sup>. It should be noted that this non-aqueous pathway yield may have large uncertainties because the 2-MT formation rate coefficients in the aqueous phase (i.e.,  $k_{H+}$ ) were determined in a bulk solution<sup>62</sup>. Recently, Zhang et al. showed that these coefficients may have been greatly over-estimated<sup>63</sup>, so the non-aqueous yield determined in this study may represent a lower bound estimate. The photooxidation reactions of 2-MT and 2-MG with OH radicals in the gas phase and aqueous phase are considered and fully evaluated in this study. A



more detailed description of the schemes is included in Supplementary Note 2: *The formation, gas-particle partitioning, and removal of 2-MT and 2-MG*. The parameters related to the partitioning and reaction kinetics<sup>34–36</sup> of 2-MT and 2-MG are summarized in Table 1.

The tracer formation, partitioning, and decay schemes described above were implemented in the CMAQv5.0.1 with 6<sup>th</sup> version of the aerosol module (AERO6). The modified model was applied to simulate the 2-MT and 2-MG for three field campaigns: summer of 2013 in the US, summer of 2012 in China, and spring of 2015 in China and the West Pacific Ocean. Detailed information about the model inputs is described in Supplementary Note 3: *General information about the model setup*. The simulations conducted to evaluate the impact of the reaction rates and phase partitioning constants in this study are listed in Supplementary Table 4.

## DATA AVAILABILITY

The SOAS observation data are publicly available from <https://csl.noaa.gov/groups/csl7/measurements/2013senex>. The observations of 2-MT and 2-MG at the PRD, 14-sites in China, and over the West Pacific, and the CMAQ source code with updated 2-MT and 2-MG mechanism are available from the Texas Data Repository (<https://doi.org/10.18738/T8/XB5XV4>).

Received: 21 November 2022; Accepted: 6 June 2023;

Published online: 17 June 2023

## REFERENCES

- Guenther, A. et al. Estimates of global terrestrial isoprene emissions using MEGAN (Model of Emissions of Gases and Aerosols from Nature). *Atmos. Chem. Phys.* **6**, 3181–3210 (2006).
- Kroll, J. H., Ng, N. L., Murphy, S. M., Flagan, R. C. & Seinfeld, J. H. Secondary organic aerosol formation from isoprene photooxidation. *Environ. Sci. Technol.* **40**, 1869–1877 (2006).
- Kroll, J. H., Ng, N. L., Murphy, S. M., Flagan, R. C. & Seinfeld, J. H. Secondary organic aerosol formation from isoprene photooxidation under high-NO<sub>x</sub> conditions. *Geophys. Res. Lett.* **32**, L18808 (2005).
- Kleindienst, T. E., Lewandowski, M., Offenberg, J. H., Jaoui, M. & Edney, E. O. Ozone-isoprene reaction: Re-examination of the formation of secondary organic aerosol. *Geophys. Res. Lett.* **34**, L01805 (2007).
- Ng, N. et al. Secondary organic aerosol (SOA) formation from reaction of isoprene with nitrate radicals (NO<sub>3</sub>). *Atmos. Chem. Phys.* **8**, 4117–4140 (2008).
- Song, M. et al. The influence of OH concentration on SOA formation from isoprene photooxidation. *Sci. Total Environ.* **650**, 951–957 (2019).
- Brownwood, B. et al. Gas-particle partitioning and SOA yields of organonitrate products from NO<sub>3</sub>-initiated oxidation of isoprene under varied chemical regimes. *ACS Earth Space Chem.* **5**, 785–800 (2021).
- Marais, E. A. et al. Aqueous-phase mechanism for secondary organic aerosol formation from isoprene: application to the southeast United States and co-benefit of SO<sub>2</sub> emission controls. *Atmos. Chem. Phys.* **16**, 1603–1618 (2016).
- Surratt, J. D. et al. Reactive intermediates revealed in secondary organic aerosol formation from isoprene. *Proc. Natl. Acad. Sci.* **107**, 6640–6645 (2010).
- Lin, Y.-H. et al. Epoxide as a precursor to secondary organic aerosol formation from isoprene photooxidation in the presence of nitrogen oxides. *Proc. Natl. Acad. Sci.* **110**, 6718–6723 (2013).
- Ying, Q., Li, J. & Kota, S. H. Significant Contributions of Isoprene to Summertime Secondary Organic Aerosol in Eastern United States. *Environ. Sci. Technol.* **49**, 7834–7842 (2015).
- Couvidat, F. & Seigneur, C. Modeling secondary organic aerosol formation from isoprene oxidation under dry and humid conditions. *Atmos. Chem. Phys.* **11**, 893–909 (2011).
- Lamkaddam, H. et al. Large contribution to secondary organic aerosol from isoprene cloud chemistry. *Sci. Adv.* **7**, eabe2952 (2021).
- Claeys, M. et al. Formation of secondary organic aerosols through photooxidation of isoprene. *Science* **303**, 1173–1176 (2004).
- Jaoui, M. et al. Formation of organic tracers for isoprene SOA under acidic conditions. *Atmos. Environ.* **44**, 1798–1805 (2010).
- Kleindienst, T. E. et al. Estimates of the contributions of biogenic and anthropogenic hydrocarbons to secondary organic aerosol at a southeastern US location. *Atmos. Environ.* **41**, 8288–8300 (2007).
- Wang, Y. et al. Characterization of Secondary Organic Aerosol Tracers over Tianjin, North China during Summer to Autumn. *ACS Earth Space Chem.* **3**, 2339–2352 (2019).
- Ding, X. et al. Spatial and seasonal variations of isoprene secondary organic aerosol in China: Significant impact of biomass burning during winter. *Sci. Rep.* **6**, 1–10 (2016).
- Paulot, F. et al. Unexpected epoxide formation in the gas-phase photooxidation of isoprene. *Science* **325**, 730–733 (2009).
- Nguyen, T. B. et al. Mechanism of the hydroxyl radical oxidation of methacryloyl peroxyxynitrate (MPAN) and its pathway toward secondary organic aerosol formation in the atmosphere. *Phys., Chem., Chem., Phys.* **17**, 17914–17926 (2015).
- Lin, Y.-H. et al. Isoprene epoxydiols as precursors to secondary organic aerosol formation: acid-catalyzed reactive uptake studies with authentic compounds. *Environ., Sci. Technol.* **46**, 250–258 (2012).
- Gaston, C. J. et al. Reactive uptake of an isoprene-derived epoxydiol to submicron aerosol particles. *Environ. Sci. Technol.* **48**, 11178–11186 (2014).
- Pye, H. O. et al. Epoxide pathways improve model predictions of isoprene markers and reveal key role of acidity in aerosol formation. *Environ. Sci. Technol.* **47**, 11056–11064 (2013).
- Budisulistiorini, S. et al. Examining the effects of anthropogenic emissions on isoprene-derived secondary organic aerosol formation during the 2013 Southern Oxidant and Aerosol Study (SOAS) at the Look Rock, Tennessee ground site. *Atmos., Chem., Phys.* **15**, 8871–8888 (2015).
- Kleindienst, T., Lewandowski, M., Offenberg, J., Jaoui, M. & Edney, E. The formation of secondary organic aerosol from the isoprene+OH reaction in the absence of NO<sub>x</sub>. *Atmos., Chem., Phys.* **9**, 6541–6558 (2009).
- Zhang, H., Surratt, J., Lin, Y., Bapat, J. & Kamens, R. Effect of relative humidity on SOA formation from isoprene/NO photooxidation: enhancement of 2-methylglyceric acid and its corresponding oligoesters under dry conditions. *Atmos., Chem., Phys.* **11**, 6411–6424 (2011).
- Wang, W. et al. Formation of secondary organic aerosol marker compounds from the photooxidation of isoprene and isoprene-derived alkene diols under low-NO<sub>x</sub> conditions. *Faraday Discuss.* **165**, 261–272 (2013).
- Ye, J. et al. Near-canopy horizontal concentration heterogeneity of semivolatile oxygenated organic compounds and implications for 2-methyltetrols primary emissions. *Environ. Sci.: Atmos.* **1**, 8–20 (2021).
- Shrivastava, M. et al. Tight Coupling of Surface and In-Plant Biochemistry and Convection Governs Key Fine Particulate Components over the Amazon Rainforest. *ACS Earth Space Chem.* **6**, 380–390 (2022).
- Riva, M. et al. Increasing isoprene epoxydiol-to-inorganic sulfate aerosol ratio results in extensive conversion of inorganic sulfate to organosulfur forms: implications for aerosol physicochemical properties. *Environ. Sci. Technol.* **53**, 8682–8694 (2019).
- Yee, L. D. et al. Natural and anthropogenically influenced isoprene oxidation in southeastern United States and central Amazon. *Environ. Sci. Technol.* **54**, 5980–5991 (2020).
- Isaacman-VanWertz, G. et al. Ambient gas-particle partitioning of tracers for biogenic oxidation. *Environ. Sci. Technol.* **50**, 9952–9962 (2016).
- Xie, M., Hannigan, M. P. & Barsanti, K. C. Gas/particle partitioning of 2-methyltetrols and levoglucosan at an urban site in Denver. *Environ. Sci. Technol.* **48**, 2835–2842 (2014).
- Kessler, S. H. et al. Chemical sinks of organic aerosol: Kinetics and products of the heterogeneous oxidation of erythritol and levoglucosan. *Environ. Sci. Technol.* **44**, 7005–7010 (2010).
- Abellar, K. A., Cope, J. D. & Nguyen, T. B. Second-order kinetic rate coefficients for the aqueous-phase hydroxyl radical (OH) oxidation of isoprene-derived secondary organic aerosol compounds at 298 K. *Environ. Sci. Technol.* **55**, 13728–13736 (2021).
- Cope, J. D., Abellar, K. A., Bates, K. H., Fu, X. & Nguyen, T. B. Aqueous Photochemistry of 2-Methyltetrol and Erythritol as Sources of Formic Acid and Acetic Acid in the Atmosphere. *ACS Earth Space Chem.* **5**, 1265–1277 (2021).
- Anastasios, C. & Newberg, J. T. Sources and sinks of hydroxyl radical in sea-salt particles. *J. Geophys. Res.: Atmos.* **112**, D10306 (2007).
- Kaur, R. et al. Photooxidants from brown carbon and other chromophores in illuminated particle extracts. *Atmos. Chem. Phys.* **19**, 6579–6594 (2019).
- Herrmann, H., Hoffmann, D., Schaefer, T., Brüner, P. & Tilgner, A. Tropospheric aqueous-phase free-radical chemistry: Radical sources, spectra, reaction kinetics and prediction tools. *ChemPhysChem* **11**, 3796–3822 (2010).
- Zhang, Y.-Q. et al. Impact of anthropogenic emissions on biogenic secondary organic aerosol: observation in the Pearl River Delta, southern China. *Atmos. Chem. Phys.* **19**, 14403–14415 (2019).
- Zhang, Y.-Q. et al. Observational insights into isoprene secondary organic aerosol formation through the epoxide pathway at three urban sites from northern to southern China. *Environ. Sci. Technol.* **56**, 4795–4805 (2022).



42. Ding, X., He, Q. F., Shen, R. Q., Yu, Q. Q. & Wang, X. M. Spatial distributions of secondary organic aerosols from isoprene, monoterpenes,  $\beta$ -caryophyllene, and aromatics over China during summer. *J. Geophys. Res.: Atmos.* **119**, 11877–11891 (2014).
43. Schwantes, R. H. et al. Low-volatility compounds contribute significantly to isoprene secondary organic aerosol (SOA) under high-NO<sub>x</sub> conditions. *Atmos. Chem. Phys.* **19**, 7255–7278 (2019).
44. Sorooshian, A. et al. Aerosol and precipitation chemistry in the southwestern United States: spatiotemporal trends and interrelationships. *Atmos. Chem. Phys.* **13**, 7361–7379 (2013).
45. Qiao, X. et al. Atmospheric wet deposition of sulfur and nitrogen in Jiuzhaigou National Nature Reserve, Sichuan Province, China. *Sci. Total Environ.* **511**, 28–36 (2015).
46. Zhang, B. et al. Significant contrasts in aerosol acidity between China and the United States. *Atmos. Chem. Phys.* **21**, 8341–8356 (2021).
47. Cui, T. et al. Development of a hydrophilic interaction liquid chromatography (HILIC) method for the chemical characterization of water-soluble isoprene epoxydiol (IEPOX)-derived secondary organic aerosol. *Environ. Sci.: Process. Impacts* **20**, 1524–1536 (2018).
48. D'Ambro, E. L. et al. Chamber-based insights into the factors controlling epoxydiol (IEPOX) secondary organic aerosol (SOA) yield, composition, and volatility. *Atmos. Chem. Phys.* **19**, 11253–11265 (2019).
49. Lopez-Hilfiker, F. et al. Molecular composition and volatility of organic aerosol in the Southeastern US: implications for IEPOX derived SOA. *Environ. Sci. Technol.* **50**, 2200–2209 (2016).
50. Guo, H. et al. Fine-particle water and pH in the southeastern United States. *Atmos. Chem. Phys.* **15**, 5211–5228 (2015).
51. Zhang, Y. et al. Isoprene mixing ratios measured at twenty sites in China during 2012–2014: Comparison with model simulation. *J. Geophys. Res.: Atmos.* **125**, e2020JD033523 (2020).
52. Shen, R.-Q., Ding, X., He, Q.-F., Cong, Z.-Y. & Wang, X.-M. Seasonal variation of secondary organic aerosol tracers in Central Tibetan Plateau. *Atmos. Chem. Phys.* **15**, 8781–8793 (2015).
53. Surratt, J. D. et al. Chemical composition of secondary organic aerosol formed from the photooxidation of isoprene. *J. Phys. Chem. A* **110**, 9665–9690 (2006).
54. Carlton, A. G. et al. Synthesis of the southeast atmosphere studies: Investigating fundamental atmospheric chemistry questions. *Bull. Am. Meteorol. Soc.* **99**, 547–567 (2018).
55. Wang, Q. et al. Impact of secondary organic aerosol tracers on tracer-based source apportionment of organic carbon and PM<sub>2.5</sub>: A case study in the Pearl River Delta, China. *ACS Earth Space Chem.* **1**, 562–571 (2017).
56. Heo, J. et al. Source apportionments of PM<sub>2.5</sub> organic carbon using molecular marker Positive Matrix Factorization and comparison of results from different receptor models. *Atmos. Environ.* **73**, 51–61 (2013).
57. He, X. et al. Abundance and sources of phthalic acids, benzene-tricarboxylic acids, and phenolic acids in PM<sub>2.5</sub> at urban and suburban sites in Southern China. *ACS Earth Space Chem.* **2**, 147–158 (2018).
58. He, X. et al. Hourly measurements of organic molecular markers in urban Shanghai, China: Observation of enhanced formation of secondary organic aerosol during particulate matter episodic periods. *Atmos. Environ.* **240**, 117807 (2020).
59. Griffin, R. J., Dabdub, D. & Seinfeld, J. H. Development and initial evaluation of a dynamic species-resolved model for gas phase chemistry and size-resolved gas/particle partitioning associated with secondary organic aerosol formation. *J. Geophys. Res.: Atmos.* **110**, D05304 (2005).
60. Pankow, J. F. An absorption model of gas/particle partitioning of organic compounds in the atmosphere. *Atmos. Environ.* **28**, 185–188 (1994).
61. Liao, K. et al. A multiple linear regression model with multiplicative log-normal error term for atmospheric concentration data. *Sci. Total Environ.* **767**, 144282 (2021).
62. Eddingsaas, N. C., VanderVelde, D. G. & Wennberg, P. O. Kinetics and products of the acid-catalyzed ring-opening of atmospherically relevant butyl epoxy alcohols. *J. Phys. Chem. A* **114**, 8106–8113 (2010).
63. Zhang, J. et al. Observationally Constrained Modeling of the Reactive Uptake of Isoprene-Derived Epoxydiols under Elevated Relative Humidity and Varying Acidity of Seed Aerosol Conditions. *ACS Earth Space Chem.* **7**, 788–799 (2023).

## ACKNOWLEDGEMENTS

The authors would like to thank the Texas A&M High Performance Research Computing (<https://hprc.tamu.edu/>) for providing the computing resources essential for completing the project. M. Shrivastava and J.Z. acknowledge support from the United States Department of Energy (DOE) Office of Science, Office of Biological and Environmental Research (BER) through the Early Career Program at the Pacific Northwest National Laboratory (PNNL). PNNL is operated for the DOE by Battelle Memorial Institute under contract DE-AC06-76RL01830. J.L., T.Z., and M.Z. acknowledge funding from the National Natural Science Foundation of China (NSFC, Grant NO. 42030708). X.D. acknowledges funding from the National Natural Science Foundation of China (NSFC, Grant NO. 42177090). J.Z.Y. acknowledges funding from the National Natural Science Foundation of China (NSFC, Grant NO. 21177031 and NO. 91543130). G.I.V.W. acknowledges funding from the United States National Science Foundation Graduate Research Fellowship (#DGE 1106400). SV-TAG data from the SOAS field campaign was collected and analyzed by G.I.V.W., L.D.Y., and A.H.G., supported by the United States National Science Foundation Atmospheric Chemistry Program (#1250569 and 1243354). The instrument as deployed was developed through support from the United States Department of Energy (DOE) SBIR grant DE-SC0004698. E.A.S. acknowledges funding from the United States Environmental Protection Agency (EPA STAR grant no. 83540101).

## AUTHOR CONTRIBUTIONS

Q.Y. and J.Z.Y. designed the research. J.Z. developed the model, performed simulations, analyzed the data, and led the writing. X.D., M.Z., A.H.G., A.B.G., J.D.S., E.A.S., and J.Z.Y. provided key observation data. J.L., X.H., T.Z., G.I.V.W., L.Y., H.Z., P.M., and S.H.B., contributed to the collection of the observation data. J.Z., M.C., Q.Y., and J.Z.Y. contributed to the additional simulations and revision of the manuscript. All authors contributed significant comments and editing of the paper.

## COMPETING INTERESTS

The authors declare no competing interests.

## ADDITIONAL INFORMATION

**Supplementary information** The online version contains supplementary material available at <https://doi.org/10.1038/s41612-023-00394-3>.

**Correspondence** and requests for materials should be addressed to Jian Zhen Yu or Qi Ying.

**Reprints and permission information** is available at <http://www.nature.com/reprints>

**Publisher's note** Springer Nature remains neutral with regard to jurisdictional claims in published maps and institutional affiliations.



**Open Access** This article is licensed under a Creative Commons

Attribution 4.0 International License, which permits use, sharing, adaptation, distribution and reproduction in any medium or format, as long as you give appropriate credit to the original author(s) and the source, provide a link to the Creative Commons license, and indicate if changes were made. The images or other third party material in this article are included in the article's Creative Commons license, unless indicated otherwise in a credit line to the material. If material is not included in the article's Creative Commons license and your intended use is not permitted by statutory regulation or exceeds the permitted use, you will need to obtain permission directly from the copyright holder. To view a copy of this license, visit <http://creativecommons.org/licenses/by/4.0/>.

© The Author(s) 2023